Hierarchically Functionalized Magnetic Core/Multishell Particles and Their Postsynthetic Conversion to Polymer Capsules

Sophia Schmitt,[†,#] Martin Silvestre,[†,#] Manuel Tsotsalas,[*,†] Anna-Lena Winkler,[†] Artak Shahnas,[†] Sylvain Grosjean,[‡,∥] Fabrice Laye,[†] Hartmut Gliemann,[†] Joerg Lahann,[†] Stefan Bräse,[§,∥] Matthias Franzreb,[†] and Christof Wöll[*,†]

[†]Institute of Functional Interfaces (IFG), [§]Institute of Toxicology and Genetics (ITG), [‡]Soft Matter Synthesis Lab, Institute for Biological Interfaces (IBG), Karlsruhe Institute of Technology (KIT), Hermann-von-Helmholtz-Platz 1, 76344, Eggenstein-Leopoldshafen, Germany and [∥]Institute of Organic Chemistry (IOC), Karlsruhe Institute of Technology (KIT), Fritz-Haber-Weg 6, 76131 Karlsruhe, Germany. [#]These authors (S.S. and M.S.) contributed equally.

ABSTRACT

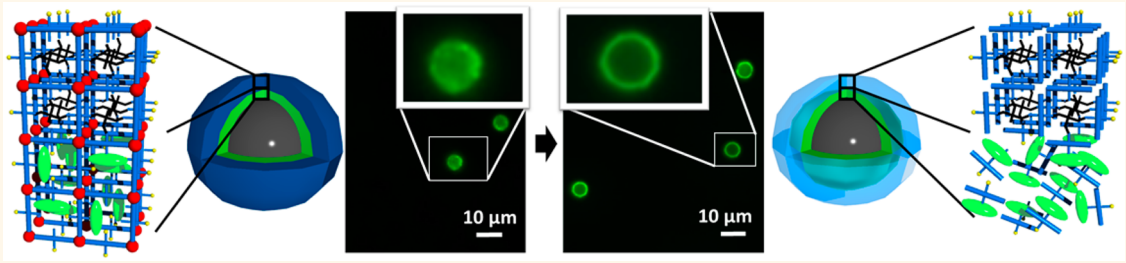

The controlled synthesis of hierarchically functionalized core/multishell particles is highly desirable for applications in medicine, catalysis, and separation. Here, we describe the synthesis of hierarchically structured metal−organic framework multishells around magnetic core particles (magMOFs) *via* layer-by-layer (LbL) synthesis. The LbL deposition enables the design of multishell systems, where each MOF shell can be modified to install different functions. Here, we used this approach to create controlled release capsules, in which the inner shell serves as a reservoir and the outer shell serves as a membrane after postsynthetic conversion of the MOF structure to a polymer network. These capsules enable the controlled release of loaded dye molecules, depending on the surrounding media.

KEYWORDS: metal−organic framework (MOF) · layer-by-layer synthesis · polymer capsules · click-chemistry · drug release

Hierarchically structured polymer capsules are of high interest for applications in biology and medicine due to their tailorable physicochemical properties combined with the ability to encapsulate and release therapeutics.[1−3] Layer-by-layer (LbL) synthesis can produce size and shape controlled capsules and tune their shell thickness and mechanical properties.[4−9] We recently presented a LbL approach for the fabrication of thin films of three-dimensionally structured gel materials (SURGELs),[10] where we use the highly ordered network of metal organic frameworks (MOF)[11,12] as a template.[13] These surface-grafted gels combine the advantages of MOF materials (highly organized molecular building blocks with various functional groups[14,15] and enormous variability in network topologies[16]) with that of polymer hydro-gels (pronounced stability against water and the absence of metal ions).[17] The SURGEL substrates showed high potential as cell culture substrate[10] as well as for electrochemical applications.[18] The ability to grow MOF shells around magnetic core particles[19] can be combined with the SURGEL approach to developed a kind of "tool box" to create highly versatile capsules containing different "loadings". Magnetic nanoparticles as a core material in the LbL synthesis offer several advantages compared to usually applied silica or polymeric particles. On the one hand, magnetic

* Address correspondence to christof.woell@kit.edu, manuel.tsotsalas@kit.edu.

Received for review January 22, 2015 and accepted March 23, 2015.

Published online March 23, 2015
10.1021/acsnano.5b00483

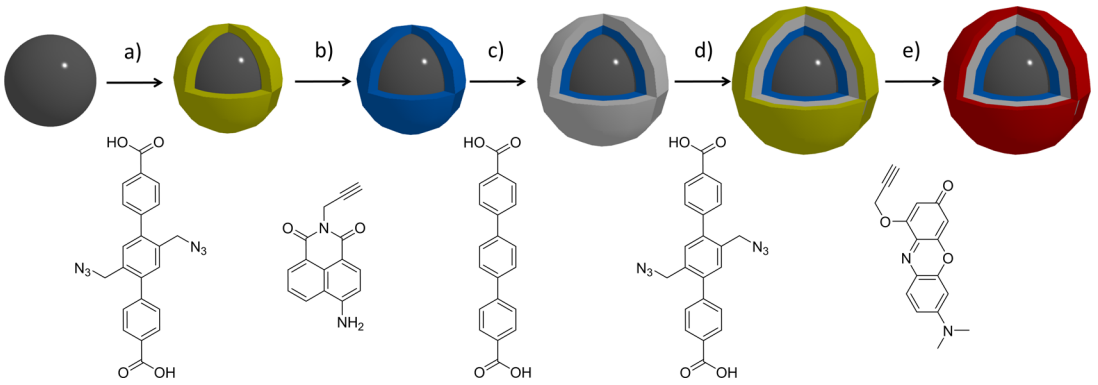

Figure 1. Shell-on-shell MOF growth around magnetic core particles after different steps. (a) MOF growth of Cu(BA-TPDC); (b) click reaction of the blue dye molecule; (c) MOF growth of Cu(TPDC); (d) MOF growth of Cu(BA-TPDC); (e) click reaction of the red dye molecule.

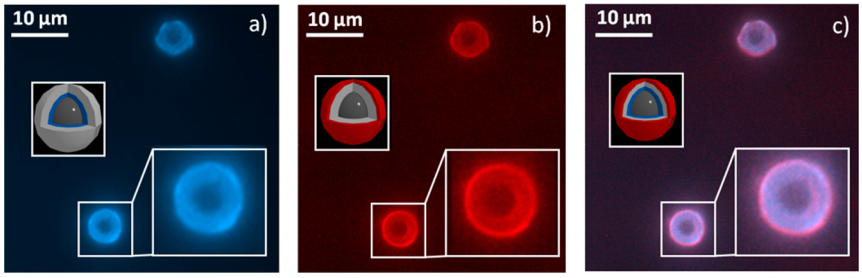

Figure 2. Confocal microscope images of the dye-functionalized multishell MOF coated nanoparticles, using different filters: (a) blue channel; (b) red channel; and (c) overlay of red/blue channel.

particles offer a simplified synthetic procedure, since the particles allow a fast and simple magnetic separation, which can be easily automated, on the other hand the magnetic properties can be used for a large variety of applications, such as hyperthermia for tumor therapies.[20]

Recently we demonstrated that LbL MOF growth is not interfered by changing the linker molecules after a desired number of cycles.[21] We used this approach to postsynthetically functionalize different MOF layers grown around magnetic particles using blue and red dye molecules.

RESULTS AND DISCUSSION

To visualize the layered structure of the MOF-shell using optical microscopy, we used micrometer sized magnetic particles with a diameter of ~5 μm. On the first five layers, realized with the terphenyldicarboxylic acid (TPDC) linker, follow 10 layers of bis(azidomethyl)-terphenyldicarboxylic acid (BA-TPDC) linker, with additional azide functionalities. We used these azide groups, to covalently attach the commercially available blue dye molecule (450-Amino Naphthalimide Alkyne) by 1,3- dipolar cycloaddition. On top of the dye-functionalized MOF-layer, we grew 16 layers of the Cu-TPDC MOF as a spacer and changed the linker again to the BA-TPDC for the last five layers (see Figure 1). The azide functionalized outer shell of the particles was functionalized with the red dye molecule (550-Red Oxazine Alkyne). Both click reactions were carried out under inert conditions in the presence of a Cu(I) catalyst.

The described four-shell MOF-on-MOF system was examined by confocal microscopy, where the inner blue and the outer red shell can be visualized (see Figure 2). This system shows the successful, homogeneous growth of a hierarchically structured multishell MOF coating around magnetic particles.

The successive formation of each layer allows a complex vertical architecture and enables us to create a multishell system, which is exploited in the following to create dye-loaded SURGEL capsules around magnetic particles. The SURGEL capsules can control the release of the encapsulated dye molecules depending on the pH of the environment.[22]

For the gel conversion we used magnetic core particles of 10 nm and 5 μm in diameter, and the MOF shell consists of the Cu-based SURMOF-2[23] network, using BA-TPDC as linker, as described above. The MOF was cross-linked with trimethylolethane tripropiolate *via* click chemistry and the copper ions of the MOF were removed by ethylenediaminetetraacetic acid (EDTA).[10] The successful coupling reaction was evidenced by infrared spectroscopy (Figure 3b) in which the azido-band at 2098 cm^{-1} from the BA-TPDC linker was substantially decreased after the coupling reaction and an alkine-band, from the cross-linker, appears at 2120 cm^{-1}. The carbonyl C═O stretching band at 1720 cm^{-1} and a C—O—C stretching band at

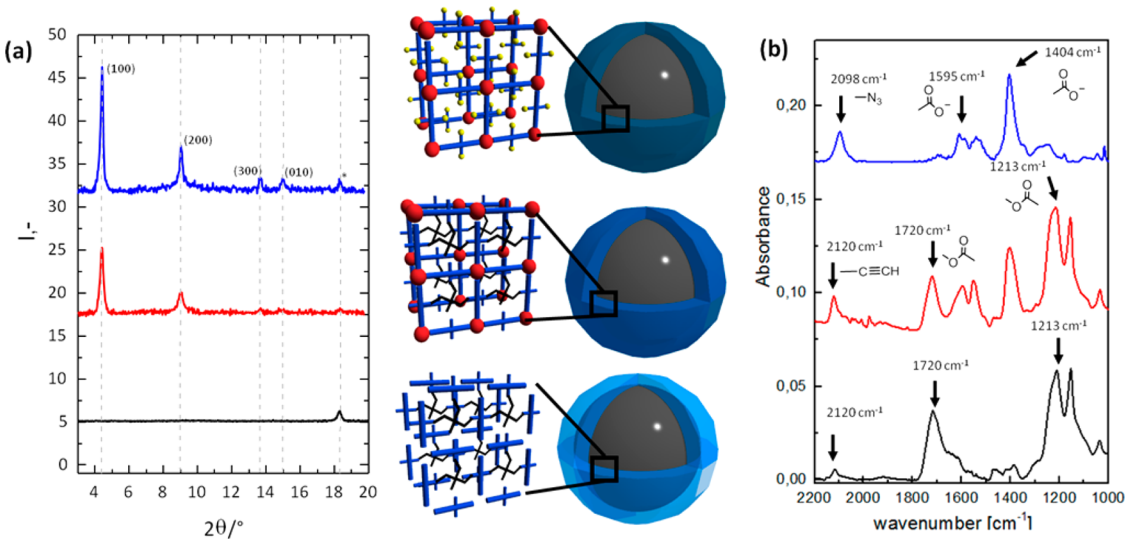

Figure 3. (a) XRD diffractograms and (b) ATR-IR spectra of the magMOF particles before (top) and after (middle) cross-linking reaction, as well as after conversion to magGEL (bottom).

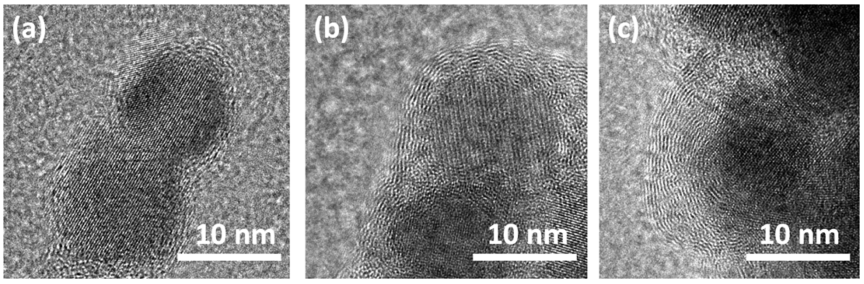

Figure 4. TEM images of magGEL particles after 10 (a), 20 (b), and 30 (c) growth cycles.

1213 cm^{-1} (both assigned to the ester-groups contained in the cross-linker) provided direct evidence for the incorporation of the linker into the SURMOF-framework.

The X-ray diffraction (XRD) data revealed the presence of highly crystalline magMOFs. The reflection peak at $2\theta = 18.3°$ is characteristic for the magnetite core particles (Fe_3O_4). As reported in a previous work on SURGEL thin films, the postsynthetic modification and cross-linking of the framework does not show any significant change in the XRD pattern, confirming that the framework structure is not changed. Upon removal of the copper ions from the cross-linked SURMOF, the structure transforms into an XRD amorphous gel (Figure 3a).[10]

We performed transmission electron microscopy (TEM) investigations with the 10 nm sized magnetic particles as core materials. These magnetic particles were coated with 10, 20, and 30 growth cycles of the MOF structures followed by cross-linking. Figure 4 shows the TEM images after the conversion to the cross-linked MagMOF and removal of the metal ions using EDTA solution. The increasing thickness and layered structure of the gel shell can be clearly seen.

A particular advantage of the liquid phase epitaxy approach is the potential for creating SURMOFs with controlled thickness and hierarchical multishell compositions.[21] The hierarchical composition gradient is of particular interest for drug delivery applications, since it gives the possibility to load inner layers of the MOF with guest molecules and coat them afterward with a protective polymer layer. Here we use this approach to create an inner magMOF layer to which we covalently attach dye molecules,[24] followed by a second magMOF layer which we use as template for the conversion into a SURGEL coating (Figure 5).

For dye loading experiments we used micrometer-sized magnetic particles to be able to investigate our system using optical microscopy. The dye loading process is based on strain-promoted azide−alkyne cycloaddition (SPAAC) between the azide functions of the MOF framework and the alkyne moiety of the commercially available Alkyne Mega Stokes dye 608 (Aldrich).[24] Figure 6 shows the fluorescence microscopy image of the magMOF particles before (6a) and after (6b) conversion to the magGEL. After gel conversion, the dye molecules are evenly distributed in the corona of the particles, since the SURGEL coatings are poorly permeable for medium sized molecules, which is consistent with our recently reported cyclic voltametry investigations where the pristine SURGEL coatings act as blocking layer.[18]

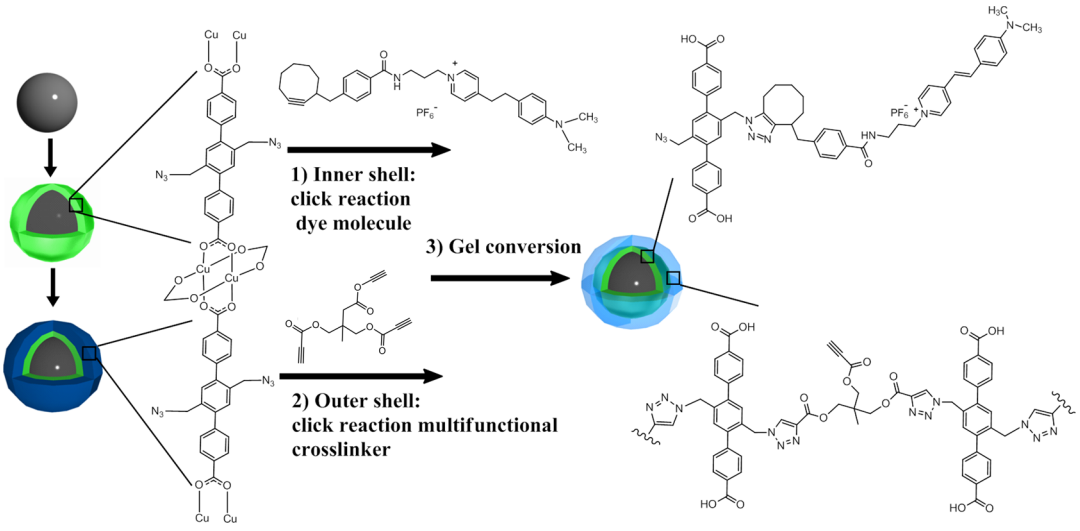

Figure 5. Schematic representation of the multistep synthesis of dye containing magGEL capsules.

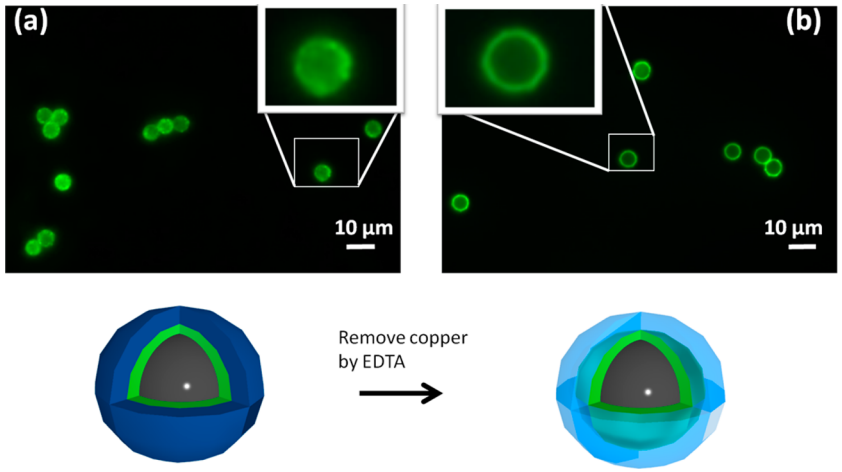

Figure 6. Fluorescence microscopy images of the cross-linked magMOF particles, respectively magGEL capsules before (a) and after (b) removal of the copper ions by EDTA.

After the conversion of the magMOF into a magGel using EDTA treatment, the dye molecules are still constrained in the inner shell of the capsules. Since the inner shell of the magMOF coating is not cross-linked (because the dye molecules used up the azide functions needed for the cross-linking) the dye molecules can float freely within the inner shell as can be seen by their more even distribution compared to before the conversion (Figure 6).

To release the dye cargo within the inner compartment of the magGEL capsules, we increased the pH of the particle suspension. The increase in the pH leads to a deprotonation of the carboxylic acid groups in the SURGEL structure, which triggers swelling of the gel shell (Figure 7a).[25,13] To study the swelling and release process, we measured the emission spectra of the solution surrounding the magGel capsules by magnetic separation of the capsules after the indicated immersion time. Figure 7b shows the emission spectra of the dye molecule released from the magGEL capsules after immersion at different pH in the range of pH 7−13 for 30 min.

As can be clearly seen from the emission spectra the dye release is triggered at pH 11 with increasing dye release upon increasing the pH to 12 and 13. In addition, we followed the release kinetics at pH 11 (Figure 7c). The release profile shows that the maximum is reached after about 120 min. This pH dependent swelling behavior can be rationalized as follows: At pH 7−10, NaOH initially diffuses easily into the gel layer. However, reaction with the carboxylic groups soon ionizes the gel, leading to the buildup of a Donnan potential which hinders the hydroxide anion from penetrating deeper into the gel. At higher pH, the Donnan potential will be diminished and NaOH will be able to diffuse easily into the gel.[26] The shift between these two mechanisms was estimated to occur in the range of solution concentrations of 10^{-3} to 10^{-2} M, or approximately pH 11−12,[27] which nicely agrees with our observed dye release profiles. From environmental

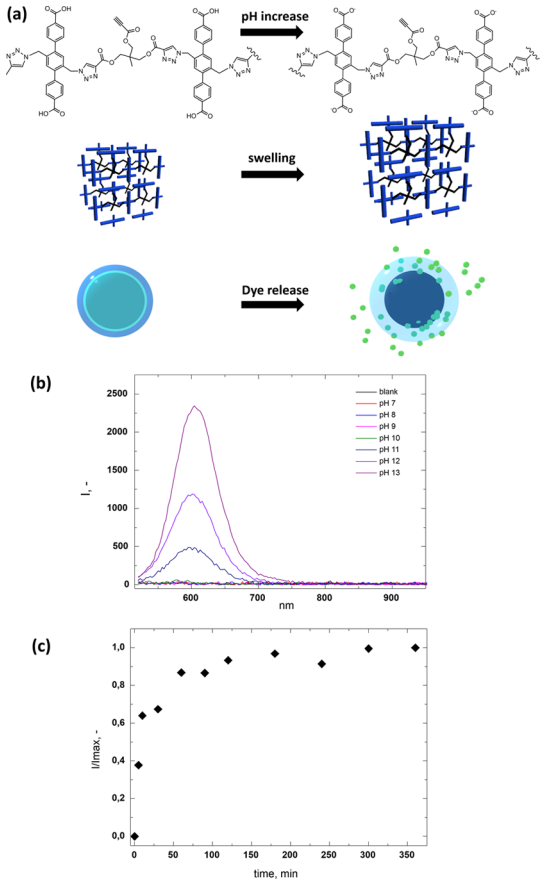

Figure 7. pH triggered dye release from magGel capsules: (a) deprotonation of the carboxylic acid groups within the shell and schematic representation of the swelling and release process; (b) emission spectra after dye release from magGEL capsules at different pH; (c) dye release kinetics at pH 11.

scanning electron microscopy (ESEM) images, after immersion at pH 11 (Supporting Information, Figure S3), no cracks or holes in the magGel shell were observed, through which the dye molecules could have left the inner compartment. These results further confirm our hypothesis that the dye release is triggered by the swelling of the SURGEL coating rather than a decomposition of the shell.

CONCLUSION

Our results demonstrate the successful fabrication of SURGEL capsules (magGELs) by growing hierarchically structured SURMOF on magnetic nanoparticles, followed by cross-linking and EDTA treatment. We also demonstrated that magGEL capsules can be prepared with controlled size and shape, and that they can be loaded with cargo molecules, for example, dye molecules, as shown in the present study. The cargo can be released from the capsules at different release kinetics depending on the pH of the environment. The release profile could be tailored to protect a loaded drug during orally administered medication. The acidic environment of the stomach is often not desired, the aim is to deliver the drug to the intestines, where the drug is released and can be absorbed to the bloodstream. The basic environment of the intestines triggers the release of the drug on the desired position.[28]

The modular approach of our gel capsule synthesis offers various possibilities to tune the network topology and their physicochemical properties by changing the linker and cross-linker structures. As we have previously shown, the SURGEL coatings can also be postsynthetically modified (PSM).[18] This PSM provides further possibilities to tune the release properties or attach bioactive molecules to the surface (e.g., antibodies or peptides[29]). Because of the modular synthesis approach, the magGEL system represents a highly versatile platform for multimodality molecular imaging[30−32] and stimuli responsive drug delivery.[33−35]

METHODS

Materials. All chemicals were purchased from commercial sources and are used without any further purification if not indicated differently. Trimethylolethane, propiolic acid, *p*-toluenesulfonic acid monohydrate and toluene were purchased from Alfa Aesar and were used as received. MagPrep-Silica particles were purchased from Merck KGaA; the surface functionalization, required for a crystalline magMOF growth, was performed as previously reported in detail.[19] In short the silica toplayer was covered by an amino-functionalized silane (APTES) using a modified Stöber method. Subsequently, glutaraldehyde was introduced as a short spacer, to obtain aldehyde functionalized particles. After repeated washing, the formyl groups were oxidized to carboxylic groups, using a 0.1 M $KMnO_4$ solution. After each step the particles were washed 3-times *via* separation of the particles with a permanent magnet. The magnetic micrometer-sized COOH functionalized particles (SiO_2-MAG-COOH) were purchased from Microparticles GmbH. In all cases, the LbL synthesis was performed in Ethanol Absolute for Analysis Emsure, purchased from VWR.

X-ray Diffraction (XRD). The XRD data were measured using a D8-Advance Bruker AXS diffractometer with Cu Kα radiation (λ = 1.5418 Å) in $\theta-\theta$ geometry and with a position sensitive detector and variable divergence slit.

Infrared (IR) Spectroscopy. For the measurements, a Bruker Optics Tensor 27 spectrometer with room temperature deuterated triglycinesulfate (RT-DTGS) detector and a Bruker Optics Platinum ATR accessory (diamond crystal with one reflection) has been applied. All spectra were recorded at room temperature (ca. 22 °C) using the software Bruker OPUS 7.2. Spectra were recorded from 4000 to 400 cm^{-1} with a resolution of 4 cm^{-1} against an air background.

Nuclear Magnetic Resonance (NMR) Spectroscopy. NMR spectra were recorded on a Bruker AM 500 spectrometer (500 MHz for ^1H/125 MHz for ^{13}C), as solutions in $CDCl_3$ or in DMSO-d_6. Chemical shifts, δ, were quoted in parts per million (ppm) and were referenced to solvent residual peak as internal standard. The following abbreviations were used to describe peak patterns when appropriate: br = broad, s = singlet, and d = doublet. Coupling constants, *J*, are reported in Hertz unit (Hz).

High Resolution Mass Spectrometry (MS and HRMS). Mass spectra were recorded with a Finnigan MAT 95 (70 eV) spectrometer under electron impact (EI) conditions. The molecular fragments were quoted as the relation between mass

and charge (m/z). The abbreviation [M^+] refers to the molecular ion.

Transmission Electron Spectroscopy (TEM) and Environmental Scanning Electron Microscope (ESEM). The TEM pictures were taken using a PHILIPS PW6061 CM200 and for the ESEM pictures a PHILIPS XL30 ESEM-FEG (Philips, Netherlands) was used.

Fluorescence Microscopy. The fluorescence images were obtained by using an Axio Observer Z1 fluorescence microscope with a Plan-APOCHROMAT 63x/1,4/oil objective and the filter set at 38 HE eGFP shift free EX BP 470/40, BS FT 495, EM BP 525/50 (Carl Zeiss, Inc., Jena, Germany).

Experimental Procedures. *Synthesis of Bis(azidomethyl)-terphenyldicarboxylic acid (BA-TPDC).* The synthetic procedure was adapted from the literature (see Supporting Information, Figure S1).[36]

Dimethyl 2′,5′-Dimethyl-[1,1′:4′,1″-terphenyl]-4,4″-dicarboxylate (1). 2,5-Dibromo-*p*-xylene (3.00 g, 11.37 mmol, 1 equiv), 4-methoxycarbonylphenylboronic acid (6.14 g, 34.10 mmol, 3 equiv), tetrakis(triphenylphosphine)palladium(0) (0.66 g, 0.57 mmol, 0.05 equiv), and sodium carbonate (9.64 g, 90.92 mmol, 8 equiv) were added in a degassed mixture of toluene−dioxane−water (450 mL, 2/2/1) under argon. The mixture was refluxed for 72 h under argon. The reaction mixture was cooled to room temperature, and organic solvents were removed under reduced pressure. The resulting aqueous suspension was extracted with dichloromethane. The organic phase was washed with water and brine, then dried over magnesium sulfate and evaporated under reduced pressure. The residue was purified with column chromatography (silica gel, dichloromethane/*n*-hexane) to give (**1**) as a white solid (2.29 g, 54%). ^{1}H NMR (500 MHz, $CDCl_3$): δ = 8.11 (d, 4H, J = 8.5 Hz, CH_{Ar}), 7.45 (d, 4H, J = 8.5 Hz, CH_{Ar}), 7.16 (s, 2H, CH_{Ar}), 3.96 (s, 6H, CO_2CH_3), 2.28 (s, 6H, $ArCH_3$) ppm. ^{13}C NMR (125 MHz, $CDCl_3$): δ = 167.1 (CO_2CH_3), 146.4 (C^{IV}), 140.5 (C^{IV}), 132.8 (C^{IV}), 131.8 (CH_{Ar}), 129.6 (C^{IV}), 129.4 (CH_{Ar}), 128.8 (CH_{Ar}), 52.2 (CO_2CH_3), 19.9 ($ArCH_3$) ppm. IR (ATR): ν = 2991, 2945, 1713, 1608, 1519, 1492, 1437, 1385, 1279, 1193 cm^{-1}. MS (EI) m/z = 374 [M^+], 343 [M^+-OCH_3], 315 [M^+-CO_2CH_3]. HRMS (EI) m/z calcd for $C_{24}H_{22}O_4$, 374.1518; found, 374.1519.

Dimethyl 2′,5′-Bis(bromomethyl)-[1,1′:4′,1″-terphenyl]-4,4″-dicarboxylate (2). Compound (**1**) (1.20 g, 3.21 mmol, 1 equiv) and *N*-bromosuccinimide (NBS) (1.26 g, 7.05 mmol, 2.2 equiv) were dissolved in benzene (60 mL). After argon bubbling for 30 min benzoyl peroxide (16 mg, 0.06 mmol, 0.02 equiv) was added, and the mixture was refluxed for 24 h. The reaction mixture was cooled to room temperature and concentrated under reduced pressure. The residue was treated with methanol and filtrated to give (**2**) as a white solid (1.66 g, 97%). ^{1}H NMR (500 MHz, $CDCl_3$): δ = 8.16 (d, 4H, J = 8.0 Hz, CH_{Ar}), 7.58 (d, 4H, J = 8.0 Hz, CH_{Ar}), 7.44 (s, 2H, CH_{Ar}), 4.42 (s, 4H, $ArCH_2Br$), 3.97 (s, 6H, CO_2CH_3) ppm. ^{13}C NMR (125 MHz, $CDCl_3$): δ = 166.9 (CO_2CH_3), 143.9 (C^{IV}), 141.4 (C^{IV}), 135.8 (C^{IV}), 133.0 (CH_{Ar}), 129.9 (CH_{Ar}), 129.8 (C^{IV}), 129.2 (CH_{Ar}), 52.2 (CO_2CH_3), 30.9 ($ArCH_2Br$) ppm. IR (ATR): ν = 2946, 1710, 1610, 1490, 1413, 1388, 1276, 1191 cm^{-1}. MS (EI) m/z = 534−532−530 [M^+], 453−451 [M^+ − Br]. HRMS (EI) m/z calcd for $C_{24}H_{20}Br_2O_4$, 529.9728; found, 529.9727.

Dimethyl 2′,5′-Bis(azidomethyl)-[1,1′:4′,1″-terphenyl]-4,4″-dicarboxylate (3). Compound (**2**) (0.75 g, 1.41 mmol, 1 equiv) and sodium azide (0.19 g, 2.96 mmol, 2.1 equiv) were dissolved in dry DMF (30 mL) and the mixture was stirred at 60 °C for 4 h under argon. The reaction mixture was cooled to room temperature, then diluted with a large amount of ethyl acetate, washed with brine, then with water. The organic layer was dried over sodium sulfate and evaporated to give (**3**) as a white solid (0.63 g, 98%). ^{1}H NMR (500 MHz, $CDCl_3$): δ = 8.15 (d, 4H, J = 8.5 Hz, CH_{Ar}), 7.49 (d, 4H, J = 8.5 Hz, CH_{Ar}), 7.43 (s, 2H, CH_{Ar}), 4.33 (s, 4H, $ArCH_2N_3$), 3.97 (s, 6H, CO_2CH_3) ppm. ^{13}C NMR (125 MHz, $CDCl_3$): δ = 166.9 (CO_2CH_3), 144.0 (C^{IV}), 141.2 (C^{IV}), 133.3 (C^{IV}), 131.6 (CH_{Ar}), 130.0 (CH_{Ar}), 129.9 (C^{IV}), 129.4 (CH_{Ar}), 52.4 (CO_2CH_3), 52.3 ($ArCH_2N_3$) ppm. IR (ATR): ν = 2953, 2088, 1716, 1607, 1436, 1338, 1272, 1180 cm^{-1}. MS (EI) m/z = 456 [M^+], 428 [M^+-N_2]. HRMS (EI) m/z calcd for $C_{24}H_{20}N_6O_4$, 456.1546; found, 456.1548.

2′,5′-Bis(azidomethyl)-[1,1′:4′,1″-terphenyl]-4,4″-dicarboxylic Acid (BA-TPDC). Compound (**3**) (0.30 g, 0.66 mmol, 1 equiv) was dissolved in tetrahydrofuran (10 mL). A saturated aqueous solution of potassium hydroxide (10 mL) was added, and the reaction mixture was stirred at room temperature for 72 h. The tetrahydrofuran was evaporated under reduced pressure, then 1 M HCl aqueous solution was added until pH = 1. The reaction mixture was extracted several times with ethyl acetate, then the organic layers were combined, washed with water and brine, dried over magnesium sulfate, and evaporated to give **BA-TPDC** as a pale yellow solid (0.27 g, 95%). ^{1}H NMR (500 MHz, DMSO-d_6): δ = 12.95 (br-s, 2H, CO_2H), 8.07 (d, 4H, J = 8.5 Hz, CH_{Ar}), 7.57 (d, 4H, J = 8.5 Hz, CH_{Ar}), 7.55 (s, 2H, CH_{Ar}), 4.50 (s, 4H, $ArCH_2N_3$) ppm. ^{13}C NMR (125 MHz, DMSO-d_6): δ = 167.1 (CO_2H), 143.4 (C^{IV}), 140.4 (C^{IV}), 133.2 (C^{IV}), 131.8 (CH_{Ar}), 130.1 (C^{IV}), 129.5 (CH_{Ar}), 129.2 (CH_{Ar}), 51.3 ($ArCH_2N_3$) ppm. IR (ATR): ν = 2921, 2853, 2090, 1681, 1606, 1565, 1458, 1317, 1285, 1235 cm^{-1}. MS (EI) m/z = 428 [M^+], 399 [M^+ − H − N_2], 386 [M^+ − N_3], 372 [M^+ − N_4], 341 [M^+ − CO_2H − N_3]. HRMS (EI) m/z calcd for $C_{22}H_{16}N_6O_4$, 428.1233; found, 428.1237.

Synthesis of Trimethylolethane Tripropiolate. The synthetic procedure was adapted from the literature.[37] In a dry 250 mL round-bottom flask equipped with a Dean−Stark trap and magnetic stirring bar was placed trimethylolethane (1.0 g, 8.30 mmol) and *p*-toluenesulfonic acid monohydrate (160 mg, 0.83 mmol, 0.1 equiv) dissolved in dry toluene (70 mL). Propiolic acid (1.9 g, 27.4 mmol, 3.3 equiv) was added dropwise, and then the mixture was heated to reflux. After 2 h the light brown solution was cooled to room temperature, and 70 mL of ethyl acetate was added. The mixture was washed twice with 5% sodium hydroxide solution (2 × 20 mL) then with brine solution (20 mL). Thereafter the product was dried over anhydrous magnesium sulfate, filtered, and concentrated *in vacuo* yielding 2.1 g (7.61 mmol, 91%) of tripropiolate as a slightly yellow oil. ^{1}H NMR (500 MHz, DMSO-d_6): δ = 4.63 (s, 3H, C≡C*H*), 4.13 (s, 6H, CH_2O), 0.98 (s, 3H, CH_3) ppm. ^{13}C NMR (125 MHz, DMSO-d_6): δ = 152.5 (*C*═O), 80.1 (C≡*C*), 74.8 (*C*≡C), 23.1 (*C*CH_2), 15.2 (*C*CH_3) ppm. HRMS (EI) m/z calcd for $C_{14}H_{12}O_6$, 276.0684; found, 276.0686.

Synthesis of magMOF on Pretreated Particles and Subsequent GEL-Conversion. *General magMOF Synthesis Conditions.* All subsequently listed magMOF syntheses follow the same procedure that was carried out and discussed in detail by Silvestre *et al.*:[19] (1) A 2 mg sample of the respective COOH-terminated particles was immersed in 2 mL of a 2 mM [$Cu(CH_3CO_2^-)_2(H_2O)_2$] ethanol solution and stirred for 3 min at 45 °C. (2) The particles were magnetically separated and washed with 2 mL of ethanol. (3) A 2 mL sample of a 0.25 mM ethanol solution of the respective linker was added and stirred for 3 min at 45 °C. (4) The particles were magnetically separated and washed with 2 mL ethanol. (5) Steps 1−4 were repeated, until the required numbers of cycles was achieved. After synthesis all samples were characterized with X-ray diffraction (XRD).

Multishell Dye Loaded Micrometer-Sized Magnetic Particles. *5-Cycle Cu(TPDC).* The synthesis followed the procedure described above. As starting material, COOH functionalized, magnetic particles with a diameter of 5 μm were used. A 2 mM [$Cu(CH_3CO^-_2)_2(H_2O)_2$] and a 0.25 mM ethanol solution of terphenyldicarboxylic acid (TPDC) were added to the particles alternately, five times each. In between each step the particles were magnetically separated and washed with 2 mL of ethanol. For the following 10-cycle Cu(BA-TPDC), the linker solution was changed to a 0.25 mM solution of bis(azidomethyl)-terphenyldicarboxylic acid (BA-TPDC) in ethanol. The alternating addition of Cu-acetate and BA-TPDC was performed for 10 cycles; in between each step the particles were separated and washed with ethanol. After 10 cycles the particles were magnetically separated and washed three times with 2 mL of methanol.

Click Reaction with the Blue Dye Molecule. The particles with 5 layers Cu(TPDC) and 10 layers Cu(BA-TPDC) in methanol were separated magnetically and immersed in 5 mL of solution of 50 μg of the blue dye molecule 450-Amino Naphtha-(imide-alkyne) and 50 μg of the Cu(I) catalyst tetrakis(acetonitrile)copper(I) hexafluorophosphate in methanol and stirred for 24 h. The click reaction was carried out under inert conditions in argon atmosphere at room temperature.

After the click reaction was completed, the particles were magnetically separated and washed three times with 2 mL of ethanol. As a spacer between the two dye functionalized layers, the particles were subsequently coated with another 16 layers

of Cu(TPDC) on top of the blue dye functionalized layer. Therefore, the particles were alternately immersed in a 2 mM $[Cu(CH_3CO^-_2)_2(H_2O)_2]$ and a 0.25 mM (TPDC) ethanol solution, with the conditions described above in the general synthesis conditions. For the outer layer, which will be functionalized with the red dye molecule, we changed the linker again to a 0.25 mM solution of the azide functionalized (BA-TPDC) linker for the last five layers of Cu(BA-TPDC). The reaction conditions are similar to the previous described conditions for the mag-MOF synthesis.

Click reaction with the red dye molecule: To functionalize the particles with the red dye molecule, the previous described particles were washed three times in methanol and immersed in 5 mL of a solution of 50 μg 550-Red Oxazine Alkyne and 50 μg of the Cu(I) catalyst tetrakis(acetonitrile)copper(I) hexafluorophosphate in methanol and stirred for 24 h at room temperature. The reaction was carried out under inert conditions in an argon atmosphere. After the reaction the particles were magnetically separated and washed three times with ethanol.

Dye-Loaded Micrometer Sized magGEL Capsules. *Cu-BA-TPDC (a).* The synthesis followed the procedure described in Supporting Information, Figure S2. As starting material, COOH functionalized micrometer-sized particles were used. A 2 mM $[Cu(CH_3CO^-_2)_2(H_2O)_2]$ and a 0.25 mM BA-TPDC ethanol solution were added to the particles alternately. After each step, the particles were washed with 2 mL of ethanol. After 10 cycles, the particles were magnetically separated and washed three times with 2 mL of ethanol.

Dye Loading (b). The dye loading process based on a strain-promoted metal-free click reaction, azide−alkyne cycloaddition (SPAAC) was carried out as described previously.[24] For the dye loading the Cu(BA-TPDC) coated particles were washed two times with toluene and added to a solution of 0.1 mg of Alkyne Mega Stokes dye 608 (Aldrich) in 10 mL of toluene. The reaction mixture was sealed and placed in an oven for 2 days at 50 °C. After synthesis the particles were magnetically separated and washed four times with 2 mL of ethanol.

Cu-BA-TPDC (c). To grow the second MOF-shell, the thoroughly washed dye-loaded Cu(BA-TPDC) particles were immersed in 2 mL of ethanol and coated with another 20 cycles Cu(BA-TPDC), using the approach described above, using a 2 mM $[Cu(CH_3CO^-_2)_2(H_2O)_2]$ and a 0.25 mM BA-TPDC ethanol solution. After 20 cycles, the particles were separated magnetically and washed with 2 mL of ethanol.

Cross-Linking Reaction (d). Freshly prepared samples of Cu(BA-TPDC) were immersed in a solution of toluene, containing 1 mg/mL trimethylolethane tripropiolate (cross-linker). The samples were heated in the solution for 7 days at 80 °C in the dark, under nitrogen atmosphere. Afterward the samples were thoroughly washed with ethanol and dried under nitrogen flow.

Conversion of the Cross-Linked magMOF into magGEL (e). Cross-linked magMOF samples were immersed in 10 mL of solution of ethanol/water in a ratio 1/1 (volume), containing 1 mg of ethylene diaminetetraacetic acid (EDTA). After 30 min immersion at room temperature, the samples were rinsed thoroughly with ethanol and water and dried under nitrogen flow.

Nanoparticles for Transmission Electron Spectroscopy (TEM). *Cu(BA-TPDC).* The synthesis followed the procedure described above. A 2 mg sample of COOH-functionalized magnetic nanoparticles was immersed in ethanol, a 2 mM $[Cu(CH_3CO_2)_2(H_2O)_2]$ and a 0.25 mM BA-TPDC ethanol solution were added to the particles alternately; in between each step the particles were washed with 2 mL of ethanol. After 10, 20, and 30 layers, the particles were separated, washed, and characterized with TEM spectroscopy. Cross-linking and conversion of cross-linked magMOF into magGEL followed parts d and e in the previous section.

Conflict of Interest: The authors declare no competing financial interest.

Acknowledgment. We thank the Interreg-program CHIRANET for the financial support.

Supporting Information Available: Additional material characterization and figures. This material is available free of charge via the Internet at http://pubs.acs.org.

REFERENCES AND NOTES

1. Cui, J.; van Koeverden, M. P.; Müllner, M.; Kempe, K.; Caruso, F. Emerging Methods for the Fabrication of Polymer Capsules. *Adv. Coloid Interface Sci.* **2014**, *207*, 14–31.
2. Richardson, J. J.; Liang, K.; Kempe, K.; Ejima, H.; Cui, J.; Caruso, F. Immersive Polymer Assembly on Immobilized Particles for Automated Capsule Preparation. *Adv. Mater.* **2013**, *25*, 6874–6878.
3. Becker, A. L.; Johnston, A. P. R.; Caruso, F. Layer-by-Layer-Assembled Capsules and Films for Therapeutic Delivery. *Small* **2010**, *6*, 1836–1852.
4. Donath, E.; Sukhorukov, G. B.; Caruso, F.; Davis, S. A.; Möhwald, H. Novel Hollow Polymer Shells by Colloid-Templated Assembly of Polyelectrolytes. *Angew. Chem., Int. Ed.* **1998**, *37*, 2201–2205.
5. De Koker, S.; Hoogenboom, R.; De Geest, B. G. Polymeric Multilayer Capsules for Drug Delivery. *Chem. Soc. Rev.* **2012**, *41*, 2867–2884.
6. Schneider, G.; Decher, G. From Functional Core/Shell Nanoparticles Prepared *via* Layer-by-Layer Deposition to Empty Nanospheres. *Nano Lett.* **2004**, *4*, 1833–1839.
7. Shimoni, O.; Yan, Y.; Wang, Y.; Caruso, F. Shape-Dependent Cellular Processing of Polyelectrolyte Capsules. *ACS Nano* **2012**, *7*, 522–530.
8. Elsner, N.; Kozlovskaya, V.; Sukhishvili, S. A.; Fery, A. pH-Triggered Softening of Crosslinked Hydrogen-Bonded Capsules. *Soft Mater.* **2006**, *2*, 966–972.
9. Such, G. K.; Tjipto, E.; Postma, A.; Johnston, A. P. R.; Caruso, F. Ultrathin, Responsive Polymer Click Capsules. *Nano Lett.* **2007**, *7*, 1706–1710.
10. Tsotsalas, M.; Liu, J.; Tettmann, B.; Grosjean, S.; Shahnas, A.; Wang, Z.; Azucena, C.; Addicoat, M.; Heine, T.; Lahann, J.; *et al*. Fabrication of Highly Uniform Gel Coatings by the Conversion of Surface-Anchored Metal−Organic Frameworks. *J. Am. Chem. Soc.* **2013**, *136*, 8–11.
11. Kitagawa, S.; Kitaura, R.; Noro, S. Functional Porous Coordination Polymers. *Angew. Chem., Int. Ed.* **2004**, *43*, 2334–2375.
12. Furukawa, H.; Cordova, K. E.; O'Keeffe, M.; Yaghi, O. M. The Chemistry and Applications of Metal−Organic Frameworks. *Science* **2013**, *341*, 1230444.
13. Ishiwata, T.; Furukawa, Y.; Sugikawa, K.; Kokado, K.; Sada, K. Clickable" Metal−Organic Framework. *J. Am. Chem. Soc.* **2013**, *135*, 5427–5432.
14. Eddaoudi, M.; Kim, J.; Rosi, N.; Vodak, D.; Wachter, J.; O'Keeffe, M.; Yaghi, O. M. Systematic Design of Pore Size and Functionality in Isoreticular MOFs and Their Application in Methane Storage. *Science* **2002**, *295*, 469–472.
15. Guillerm, V.; Kim, D.; Eubank, J. F.; Luebke, R.; Liu, X.; Adil, K.; Lah, M. S.; Eddaoudi, M. A Supermolecular Building Approach for the Design and Construction of Metal−organic Frameworks. *Chem. Soc. Rev.* **2014**, *43*, 6141–6172.
16. Deng, H.; Grunder, S.; Cordova, K. E.; Valente, C.; Furukawa, H.; Hmadeh, M.; Grandara, F.; Whalley, A. C.; Liu, Z.; Asahina, S.; *et al*. Large-Pore Apertures in a Series of Metal-Organic Frameworks. *Science* **2012**, *336*, 1018–1023.
17. Deng, X.; Friedmann, C.; Lahann, J. Bio-orthogonal "Double-Click" Chemistry Based on Multifunctional Coatings. *Angew. Chem., Int. Ed.* **2011**, *50*, 6522–6526.
18. Mugnaini, V.; Tsotsalas, M.; Bebensee, F.; Grosjean, S.; Shahnas, A.; Bräse, S.; Lahann, J.; Buck, M.; Wöll, C. Electrochemical Investigation of Covalently Postsynthetic Modified SURGEL Coatings. *Chem. Commun.* **2014**, *50*, 11129–11131.
19. Silvestre, E.; Franzreb, M.; Weidler, P. G.; Shekhah, O.; Wöll, C. Magnetic Nanoparticles: Magnetic Cores with Porous Coatings: Growth of Metal−Organic Frameworks on Particles Using Liquid Phase Epitaxy. *Adv. Funct. Mater.* **2013**, *23*, 1093–1093.
20. Kumar, C. S.; Mohammad, F. Magnetic Nanomaterials for Hyperthermia-Based Therapy and Controlled Drug Delivery. *Adv. Drug Delivery Rev.* **2011**, *63*, 789.
21. Wang, Z.; Liu, J.; Lukose, B.; Gu, Z.; Weidler, P. G.; Gliemann, H.; Heine, T.; Wöll, C. Nanoporous Designer Solids with Huge Lattice Constant Gradients: Multiheteroepitaxy of

Metal−Organic Frameworks. *Nano Lett.* **2014**, *14*, 1526–1529.
22. Delcea, M.; Möhwald, H.; Skirtach, A. G. Stimuli-Responsive LbL capsules and nanoshells for drug delivery. *Adv. Drug Delivery Rev.* **2011**, *63*, 730–747.
23. Liu, J.; Lukose, B.; Shekhah, O.; Arslan, H. K.; Weidler, P.; Gliemann, H.; Bräse, S.; Grosjean, S.; Godt, A.; Feng, X.; *et al.* A novel series of isoreticular metal organic frameworks: realizing metastable structures by liquid phase epitaxy. *Sci. Rep.* **2012**, *2*, 1–5.
24. Wang, Z.; Liu, J.; Arslan, H. K.; Grosjean, S.; Hagendorn, T.; Gliemann, H.; Bräse, S.; Wöll, C. Postsynthetic Modification of Metal−Organic Framework Thin Films Using Click Chemistry: The Importance of Strained C−C Triple Bonds. *Langmuir* **2013**, *29*, 15958–15964.
25. Ricka, J.; Tanaka, T. Swelling of Ionic Gels: Quantitative Performance of the Donnan Theory. *Macromolecules* **1984**, *17*, 2916–2921.
26. Gehrke, S. H.; Cussler, E. L. Mass Transfer in pH-Sensitive Hydrogels. *Chem. Eng. Sci.* **1989**, *44*, 559–566.
27. Helfferich, F. Ion-Exchange Kinetics. V. Ion Exchange Accompanied by Reactions. *J. Phys. Chem.* **1965**, *69*, 1178–1187.
28. Peppas, N. A.; Huang, Y.; Torres-Lugo, M.; Ward, J. H.; Zhang, J. Physicochemical Foundations and Structural Design of Hydrogels in Medicine and Biology. *Annu. Rev. Biomed. Eng.* **2000**, *2*, 9–29.
29. Sapsford, K. E.; Algar, W. R.; Berti, L.; Gemmill, K. B.; Casey, B. J.; Oh, E.; Stewart, M. H.; Medintz, I. L. Functionalizing Nanoparticles with Biological Molecules: Developing Chemistries that Facilitate Nanotechnology. *Chem. Rev.* **2013**, *113*, 1904–2074.
30. Burns, A. A.; Vider, J.; Ow, H.; Herz, E.; Penate-Medina, O.; Baumgart, M.; Larson, S. M.; Wiesner, U.; Bradbury, M. Fluorescent Silica Nanoparticles with Efficient Urinary Excretion for Nanomedicine. *Nano Lett.* **2009**, *9*, 442–448.
31. Tsotsalas, M.; Kopka, K.; Luppi, G.; Wagner, S.; Law, M.; Schäfer, M.; De Cola, L. Encapsulating ^{111}In in Nanocontainers for Scintigraphic Imaging: Synthesis, Characterization, and in Vivo Biodistribution. *ACS Nano* **2010**, *4*, 342–348.
32. Tsotsalas, M.; Busby, M.; Gianolio, E.; Aime, S.; De Cola, L. Functionalized Nanocontainers as Dual Magnetic and Optical Probes for Molecular Imaging Applications. *Chem. Mater.* **2008**, *20*, 5888–5893.
33. Horcajada, P.; Chalati, T.; Serre, C.; Gillet, B.; Sebrie, C.; Baati, T.; Eubank, J. F.; Heurtaux, D.; Clayette, P.; Kreuz, C.; *et al.* Porous Metal−Organic-Framework Nanoscale Carriers as a Potential Platform for Drug Delivery and Imaging. *Nat. Mater.* **2010**, *9*, 172–178.
34. Khaletskaya, K.; Reboul, J.; Meilikhov, M.; Nakahama, M.; Diring, S.; Tsujimoto, M.; Isoda, S.; Kim, F.; Kamei, K.; Fischer, R. A.; *et al.* Integration of Porous Coordination Polymers and Gold Nanorods into Core−Shell Mesoscopic Composites toward Light-Induced Molecular Release. *J. Am. Chem. Soc.* **2013**, *135*, 10998–11005.
35. Argyo, C.; Weiss, V.; Bräuchle, C.; Bein, T. Multifunctional Mesoporous Silica Nanoparticles as a Universal Platform for Drug Delivery. *Chem. Mater.* **2014**, *26*, 435–451.
36. Barral, K.; Moorhouse, A. D.; Moses, J. E. Efficient Conversion of Aromatic Amines into Azides: A One-Pot Synthesis of Triazole Linkages. *Org. Lett.* **2007**, *9*, 1809–1811.
37. Gorman, I. E.; Willer, R. L.; Kemp, L. K.; Storey, R. F. Development of a Triazole-Cure Resin System for Composites: Evaluation of Alkyne Curatives. *Polymer* **2012**, *53*, 2548–2558.